

ChemComm

Chemical Communications

Accepted Manuscript

This article can be cited before page numbers have been issued, to do this please use: B. N. Sanchez Eguia, A. Company, M. Costas and J. Serrano-Plana, *Chem. Commun.*, 2020, DOI: 10.1039/D0CC05942K.



This is an Accepted Manuscript, which has been through the Royal Society of Chemistry peer review process and has been accepted for publication.

Accepted Manuscripts are published online shortly after acceptance, before technical editing, formatting and proof reading. Using this free service, authors can make their results available to the community, in citable form, before we publish the edited article. We will replace this Accepted Manuscript with the edited and formatted Advance Article as soon as it is available.

You can find more information about Accepted Manuscripts in the [Information for Authors](#).

Please note that technical editing may introduce minor changes to the text and/or graphics, which may alter content. The journal's standard [Terms & Conditions](#) and the [Ethical guidelines](#) still apply. In no event shall the Royal Society of Chemistry be held responsible for any errors or omissions in this Accepted Manuscript or any consequences arising from the use of any information it contains.

COMMUNICATION

Catalytic O₂ activation with synthetic models of α-ketoglutarate dependent oxygenasesBrenda N. Sánchez-Eguía,^a Joan Serrano-Plana,^a Anna Company,^{*a} Miquel Costas^{*a}Received 00th January 20xx,
Accepted 00th January 20xx

DOI: 10.1039/x0xx00000x

An iron complex bearing the facially capping tridentate 1,4,7-triazacyclononane ligand mimics structural and functional features of alpha-ketoglutarate (α-KG) dependent enzymes, and engages in enzyme-like catalytic O₂ activation coupled to α-cetoacid decarboxylation, oxygenating sulfides. This system constitutes a rare case of non-enzymatic catalytic O₂ activation, cycling between Fe^{II} and Fe^{IV}(O).

O₂ activation is a long standing problem in bioinorganic chemistry and in catalysis.¹⁻⁶ O₂ is often incorporated into autooxidation, free-radical chains, but its use to generate metal-based oxygen atom transfer agents susceptible to engage in selective transformations in a catalytic manner is rare.

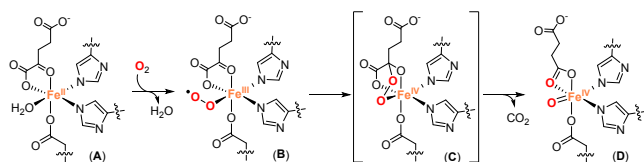


Figure 1. O₂ activation mechanism of α-KG dependent oxygenases.⁷

Several iron dependent metalloproteins catalyze O₂ activation reactions.⁸ An important class are α-ketoglutarate (α-KG) dependent enzymes, which contain a non-heme center that carries out substrate oxidation concomitantly with the oxidative decarboxylation of an α-keto carboxylate using O₂ as the oxidant.⁹⁻¹¹ X-ray diffraction (XRD) analyses of several members of this family reveal that in the active site the iron center is coordinated to the 2-histidine-1-carboxylate facial triad¹² occupying one face of the metal coordination octahedron (Figure 1, A), leaving the three extra coordination sites available for co-substrate (ketoacid) and O₂ binding. O₂ activation at this

center (Figure 1, B and C) is coupled to decarboxylation of the ketoglutarate bound ligand, and results in the formation of a Fe^{IV}-oxo species (Figure 1, D) which has been spectroscopically characterized in several members of this family,^{7,13} and it is the substrate oxidizing species.

Small molecule iron coordination complexes have contributed to the understanding of the chemistry displayed by these enzymes.¹⁴ Functional models include iron complexes bearing a tri- or tetradentate N-based ligand together with an α-KG surrogate such as benzoyl formate (BF) or pyruvate (PV).¹⁴ Reaction of these model complexes with O₂ produces oxidants that can undergo intramolecular oxidation of the ligand, or can be intercepted by an external substrate. A major standing goal has been the implementation of these O₂ activation reactions in catalytic processes but still successful examples remain very rare.¹⁵⁻¹⁷ Presumably, this reflects the difficulty in finding iron catalysts that activate O₂ and engage in a Fe^{II}-Fe^{IV} cycle, without decaying into the inactive ferric forms. In this work we describe a synthetic model of α-KG iron enzymes that overcomes this challenge and shows catalytic O₂ activation activity.

Reaction of *i*Pr₃tacn¹⁸ (Figure 2) with equimolar amounts of [Fe(CF₃SO₃)₂(CH₃CN)₂] and sodium benzoylformate (NaBF) in acetonitrile under an inert atmosphere led to the formation of the corresponding iron-benzoylformate complex [Fe(BF)(CF₃SO₃)(*i*Pr₃tacn)] (**1BF**), which was isolated as purple crystals in 76% yield after slow diffusion of ether to an acetonitrile solution of the complex (Figure 2). Analogously, but replacing NaBF by sodium benzoate (NaBz), the carboxylate complex [Fe(Bz)(*i*Pr₃tacn)(CH₃CN)](CF₃SO₃) (**1Bz**) was prepared and isolated as pale yellow crystals in 92% yield. The solid state molecular structures of **1BF** and **1Bz** (Figure 2) can be established by X-ray diffraction analysis. Most notable, the *i*Pr₃tacn ligand affords mononuclear architectures (**1BF** and **1Bz**) featuring rare cases of non-bridging ketocarboxylate and carboxylate moieties (Figure 2). The structure of **1BF** is also interesting because the BF ligand adopts the k²-chelating mode observed in several α-KG-dependent iron(II) enzymes.^{10, 19} The

^a Institut de Química Computacional i Catalysis (IQCC). Universitat de Girona. Facultat de Ciències, Campus de Montilivi, 17003, Girona, Spain.

† Footnotes relating to the title and/or authors should appear here.

Electronic Supplementary Information (ESI) available: [details of any supplementary information available should be included here]. See DOI: 10.1039/x0xx00000x

ketocarboxylate is nearly coplanar, and chelates the iron center via a carboxylate and a carbonyl O atoms (Fe–O distances of 2.039 Å and 2.215 Å, respectively).

In order to explore the impact of the steric bulk of the tacn ligand, we synthesized the less sterically encumbered *i*Bu₃tacn ligand. Several attempts to prepare iron complexes from the triflate salt proved unsuccessful. Alternatively, we assembled the [Fe(*i*Bu₃tacn)]²⁺ complex *in situ* by reacting the ligand with equimolar amounts of anhydrous FeCl₂ in acetonitrile, followed by addition of 2 equiv AgClO₄. The subsequent addition of 1 equiv NaBF gives rise to a deep brown solution. Filtration to remove the AgCl precipitate and slow diethyl ether diffusion over the resulting solution unexpectedly led to the formation of [Fe₂(BF)₂(μ-Cl)(*i*Bu₃tacn)₂](ClO₄) (**2BF-ClO₄**) as orange crystals suitable for X-ray diffraction in 74%. The peculiarity of this complex compared to **1BF** and **1Bz** is that the benzoformate is not bound in a chelate fashion and instead a carboxylate bridged (Fe–O distances are undistinguishable, ~ 2.1 Å) diiron compound is formed. Presumably, the ligand *i*Pr₃tacn, featuring tertiary alkyl sites α to the N atoms, exerts a steric protection that disfavors carboxylate bridged species. The introduction of a methylenic unit α to the N in each of the substituents of the triazacyclononane ring in *i*Bu₃tacn alleviates the steric hindrance and enables the formation of dimeric compounds.

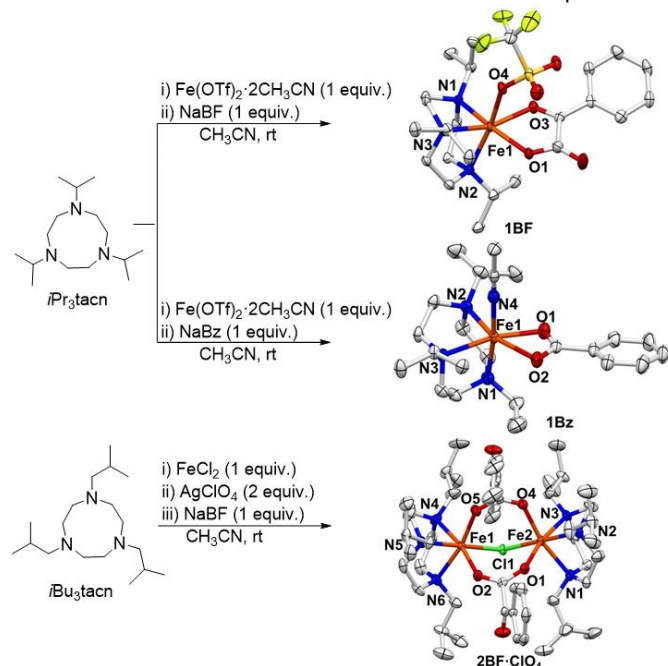


Figure 2. Chemical structure of *i*Pr₃tacn and *i*Bu₃tacn, along with X-ray structures of **1BF**, **1Bz** and **2BF-ClO₄** (CCDC 2026906-2026908). Hydrogen atoms and noncoordinating anions have been omitted for clarity.

The absorption spectra of the complexes are informative of the coordination mode of the BF ligand. The UV-Vis spectrum of **1BF** in acetonitrile exhibits broad absorption bands at 520 nm (300 M⁻¹cm⁻¹) and 570 nm (300 M⁻¹cm⁻¹), which gives **1BF** its characteristic purple color of iron(II)-bidentate α-keto acid units.^{20, 21} The origin of these absorption bands is attributed to MLCT transitions from the iron(II) center to the π* orbitals of

the chelated ketocarboxylate ligand.²² As expected, no absorption in this low energy region was detected for **1Bz**. In the case of **2BF-ClO₄** (dimeric species) the observed bridging coordination of the BF unit is expected to afford no absorption in 500–600 nm region. Nevertheless, weak bands are observed in acetonitrile in this region, suggesting that the dimeric structure may be partially broken in solution (to yield a minor amount of the k²-chelated iron complex), or alternatively, rapid oxidation to form a oxo-bridged diferric complex, which also display characteristic weak bands in this region.^{18e,23}

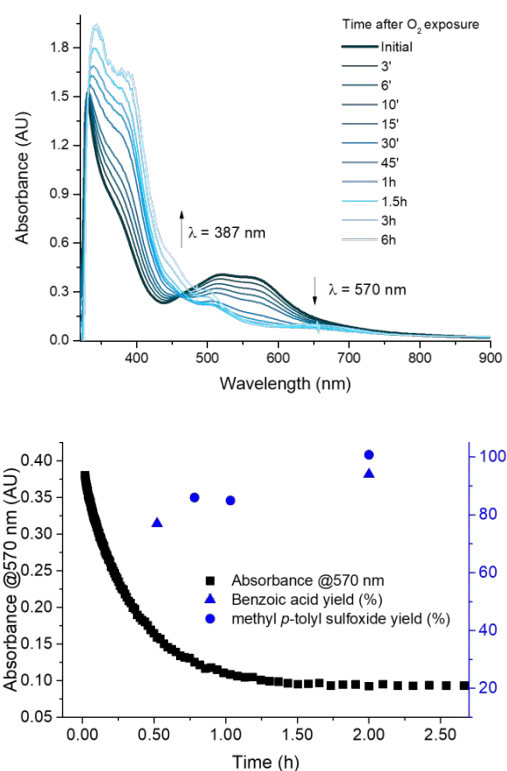


Figure 3. a) UV-vis monitoring of the reaction of **1BF** with O₂ in the presence of 100 equiv *p*-methyl tolyl sulfide in acetone at room temperature [**1BF**]₀ = 1.3 mM. b) Time trace of the decay of the band at 570 nm together with the quantification over time of the production of HBz and *p*-methyl tolyl sulfide.

Reaction of **1BF** with O₂ at room temperature was followed by means of UV-vis spectroscopy by monitoring the decay of its characteristic MLCT band at 570 nm in different solvents. The rate of decay of this band upon reaction with O₂ could be fitted to a single exponential function and it was dependent on the solvent used. While the decay was complete in about 1 h in acetone ($k_{obs} = (1.15 \pm 0.07) \times 10^{-3} \text{ s}^{-1}$, $t_{1/2} = 10 \text{ min}$), the reaction was ~5 times slower in acetonitrile ($k_{obs} = (2.62 \pm 0.02) \times 10^{-4} \text{ s}^{-1}$, $t_{1/2} = 44 \text{ min}$). ¹H-NMR analysis reveals that 0.85 and 0.8 equiv. of benzoic acid (HBz) per iron center are formed in acetone and acetonitrile, respectively. This strongly suggests that O₂ activation is coupled to α-KG decarboxylation (Figure 1). The nearly equivalent formation of benzoic acid per iron center observed upon reaction of **1BF** with O₂ in acetone and acetonitrile points towards a reaction mechanism where the

ferrous center is two-electron oxidized, analogous to the enzymatic cycle (Figure 1).

Irrespective of the solvent, attempts to trap reaction intermediates from O₂ binding were unsuccessful. However, evidence for the formation of an intermediate capable of engaging in two-electron oxygen atom transfer was gained by interception with an external substrate. Thus, **1BF** oxygenation was performed in the presence of 100 equiv methyl *p*-tolyl sulfide. GC-FID analysis after the reaction performed in acetone revealed that 0.99 equiv. methyl *p*-tolyl sulfoxide with respect to iron were formed. When the reaction was performed in acetonitrile, a similar result was obtained (0.8 equiv.). Experiments using **1Bz** or [Fe(CF₃SO₃)₂(CH₃CN)₂] instead of **1BF** did not afford any oxidized product.

The oxygenation of **2BF-CIO₄** was also studied. Reaction of the complex dissolved in acetone proceeds fast (< 10 min). ¹H-NMR analysis after reaction also revealed the formation of benzoic acid (60% yield) but in this case, benzoic acid formation was not coupled to sulfoxide production which was obtained in only 18% yield. Overall, these observations suggest that the presence of a mononuclear iron center coordinating the BF moiety in a bidentate fashion as observed in **1BF** is necessary to achieve O₂ activation reactions where a two-electron oxidant is formed.

The mechanistic model considered for the reaction of **1BF** with O₂ is based in the mechanism proposed for α-KG dependent enzymes (Figure 1); O₂ binding and activation at the iron center is coupled to decarboxylation, generating a high valent iron(IV)-oxo species that is then responsible for substrate oxidation. In order to validate this hypothesis, we monitored simultaneously the reaction of **1BF** with O₂ (UV-Vis), the production of HBz (¹H-NMR) and the formation of sulfoxide (GC). Interestingly, analysis of the HBz and sulfoxide produced over time in acetone and acetonitrile confirmed that the decarboxylation and sulfoxidation reactions occur concomitantly with the consumption of **1BF** (Figure 3 and S26). Thus, the time trace for the decomposition of **1BF** upon reaction with O₂ in the presence of a sulfide inversely correlates with the time trace corresponding to the amount of HBz and sulfoxide produced in both acetone and acetonitrile solvents, indicating that these three events are coupled. This result substantiates the hypothesis that benzoylformate oxidative decarboxylation occurs with the concomitant formation of the ferryl species, that oxidizes the sulfide, following a set of events similar to those taking place in α-KG dependent oxygenases (Figure 1). However, oxidation by a peroxide intermediate (intermediate c in Figure 1) should be also considered.²⁴

Isotope labeling experiments were used to get further insight into the reaction mechanism. Following the same procedure as above, **1BF** was reacted with ¹⁸O₂ in acetone in the presence of 100 equiv methyl *p*-tolyl sulfide. GC-MS analysis of the reaction products revealed 90% incorporation of ¹⁸O in the methyl *p*-tolyl sulfoxide product (Figure S32). Likewise, 90% ¹⁸O incorporation was found in HBz (ESI-MS, negative mode, Figure S34). The fact that both products incorporate one 18-oxygen atom aligns with the mechanism that operates in α-KG dependent oxygenases (Figure 1), where the oxygen atoms incorporated into the products originate from molecular oxygen.

The electronic nature of the reaction between the putative iron(IV)-oxo intermediate and the sulfide substrate was studied by performing competitive oxidation experiments using pairs of *p*-X-substituted methyl phenyl sulfides, (X = OCH₃, CH₃, Cl, CN, NO₂). A Hammett analysis revealed a linear correlation with a ρ value of -1.1 (Figure S29). This is indicative of the electrophilic nature of the oxidant. Similar values between -0.9 and -1.5 have been reported for the oxidation of sulfides by spectroscopically trapped iron(IV)-oxo.²⁵⁻²⁷

We obtained more indirect evidence for the formation of an iron(IV)-oxo compound by performing experiments with H₂¹⁸O. In order to do so, oxygenation of **1BF** in acetone in the presence of 100 equiv of methyl *p*-tolyl sulfide and increasing amounts of H₂¹⁸O (10 to 80 equiv, Figure S30) was carried out. GC-MS product analysis revealed a linear increment of ¹⁸O-incorporation into the sulfoxide product from 3% to 11%. The same trend was observed when the *p*-chlorophenyl derivative was used as substrate (increment of ¹⁸O incorporation from 5% to 15%). Control experiments indicated that sulfoxides do not exchange their oxygen atoms with water under the reaction conditions studied. It is known that iron(IV)-oxo species can exchange their oxo ligand with water,^{28, 29} which reinforces the idea of the formation of such compounds upon reaction of **1BF** and O₂.

The sum of the experimental evidence indicates that O₂ activation at **1BF** proceeds via a mechanism resembling α-KG-dependent oxygenases, and cycles between Fe^{II} and Fe^{IV} species. The consequence of this conclusion is that sulfide oxidation could be rendered catalytic, provided the reactions would be performed in the presence of an excess of BF. To test this hypothesis, **1BF** was reacted with O₂ in the presence of a large excess of methyl *p*-tolyl sulfide and excess of benzoylformic acid (HBF). In all cases, the equivalents of HBF dictate the maximum turnover number (TN) that can be achieved. Initially 10 equiv HBF were used in combination with 100 equiv sulfide (Table 1, entry 1) which resulted in 8 TN of the corresponding sulfoxide. Decreasing the amount of HBF to 3 equiv afforded the maximum expected TN of 3, while the use of 5 equiv HBF resulted in 4 TN of sulfoxide product (Table 1, entry 2 and 3). Further increase in the amount of HBF did not afford higher turnover numbers (6 TN when 50 equiv HBF were used or only 2.5 TN in the presence of 100 equiv HBF, Table 1 entries 5 and 6). The highest substrate conversion was achieved when 10 equiv HBF were combined with 20 equiv *p*-methyl phenyl sulfide in the presence of 10 equiv HBF, affording 6 TN of sulfoxide product that represent a notable 30% conversion of the substrate into the sulfoxide. Delivery of HBF by syringe pump did not improve product yields (see Table S3).

Although these results may be seen as modest from a synthetic perspective, they represent a very rare example of a biomimetic iron catalyzed O₂-activation reactions.³⁰⁻³² Insight into the catalyst deactivation mechanism was gained by performing an ESI-MS analysis of the reaction mixture after a catalytic reaction. The spectrum was dominated by a prominent peak at *m/z* = 256.2 corresponding to the protonated *i*Pr₃tacn ligand, suggesting that catalyst deactivation occurs via protodemetalation (Figure S36). In addition, product inhibition

was discarded because the reaction is not affected by the initial presence of a sulfoxide. Attempts to recover the catalyst after 2h of reaction by addition of reducing agents or FeOTf₂ proved unsuccessful (see Table S3 for details).

Table 1. Catalytic activation of O₂ with **1BF**

Entry	HBF (equiv.) ^a	Substrate (equiv.) ^a	TN
1	10	100	8
2	3	100	3
3	5	100	4
4	10	50	4
5	50	100	6
6	100	100	2.5
7	10	20	6

^aWith respect to **1BF**

In conclusion, the current work describes the preparation of small molecule models of the active site of α -KG-dependent enzymes and exhibit catalytic O₂ activation. Mechanistic studies suggest that the reaction of **1BF** with O₂ proceeds via a biomimetic Fe^{II}/Fe^{IV} cycle and formation of ferric species is prevented. The work also demonstrates the viability of this biologically inspired approach to activate O₂ with small molecule coordination compounds, operating via a mechanism fundamentally distinct from a free radical autooxidation process.

Conflicts of interest

“There are no conflicts to declare”.

Notes and references

‡ Footnotes relating to the main text should appear here. These might include comments relevant to but not central to the matter under discussion, limited experimental and spectral data, and crystallographic data.

1. T. Punniyamurthy, S. Velusamy and J. Iqbal, *Chem. Rev.*, 2005, **105**, 2329-2364.
2. D. Wang, A. B. Weinstein, P. B. White and S. S. Stahl, *Chem. Rev.*, 2018, **118**, 2636-2679.
3. Z. Z. Shi, C. Zhang, C. H. Tang and N. Jiao, *Chem. Soc. Rev.*, 2012, **41**, 3381-3430.
4. H. Sterckx, B. Morel and B. U. W. Maes, *Angew. Chem. Int. Ed.*, 2019, **58**, 7946-7970.
5. K. P. Bryliakov, *Chem. Rev.*, 2017, **117**, 11406-11459.
6. S. Sahu and D. P. Goldberg, *J. Am. Chem. Soc.*, 2016, **138**, 11410-11428.
7. J. C. Price, E. W. Barr, B. Tirupati, J. M. Bollinger, Jr. and C. Krebs, *Biochemistry*, 2003, **42**, 7497-7508.
8. E. G. Kovaleva and J. D. Lipscomb, *Nat. Chem. Biol.*, 2008, **4**, 186-193.
9. M. S. Islam, T. M. Leissing, R. Chowdhury, R. J. Hopkinson and C. J. Schofield, *Annual Rev. Biochem.*, 2018, **87**, 585-620.

10. M. A. McDonough, C. Loenarz, R. Chowdhury, I. J. Clifton and C. J. Schofield, *Curr. Opin. Struct. Biol.*, 2010, **20**, 659-672.
11. S.-S. Gao, N. Naowarajna, R. Cheng, X. Liu and P. Liu, *Nat. Prod. Rep.*, 2018, **35**, 792-837.
12. E. L. Hegg and L. Que, Jr. *Eur. J. Biochem.*, 1997, **250**, 625-629.
13. J. M. Bollinger, Jr., W. C. Chang, M. L. Matthews, R. J. Martinie, A. K. Boal and C. Krebs, In *RSC Metallobiology*, 2015, January, 95-122.
14. T. K. Paine and L. Que, Jr. in *Molecular Design in Inorganic Biochemistry*, ed. D. Rabinovich, Springer Berlin Heidelberg, Berlin, Heidelberg, 2014, pp. 39-56.
15. D. Sheet and T. K. Paine, *Chem. Sci.*, 2016, **7**, 5322-5331.
16. D. Sheet, A. Bera, Y. Fu, A. Desmecht, O. Riant and S. Hermans, *Chem. Eur. J.*, 2019, **25**, 9191-9196.
17. D. Sheet, P. Halder and T. K. Paine, *Angew. Chem. Int. Ed.*, 2013, **52**, 13314-13318.
18. For previous use of tacn ligands in modelling O₂-activating mononuclear iron enzymes see; a) J. B. Gordon, A. C. Vilbert, I. M. DiMucci, S. N. MacMillan, K. M. Lancaster, P. Moëne-Loccoz and D. P. Goldberg, *J. Am. Chem. Soc.*, 2019, **141**, 17533-17547. b) A. Diebold; A. Elbouadili; K. S. Hagen, *Inorg. Chem.* 2000, **39**, 3915. c) D.-H. Jo; L. Que, Jr., *Angew. Chem. Int. Ed.* 2000, **39**, 4284. d) G. Lin; G. Reid, T. D. H. Bugg, *J. Am. Chem. Soc.* 2001, **123**, 5030. e) J. R. Hartman, R. L. Rardin, P. Chaudhuri, K. Pohl, K. Wiegardt, B. Nuber, J. Weiss, G. C. Papaefthymiou, R. B. Frankel and S. J. Lippard, *J. Am. Chem. Soc.*, 1987, **109**, 7387-7396.
19. Z. Zhang, J. Ren, D. K. Stammers, J. E. Baldwin, K. Harlos and C. J. Schofield, *Nat. Struct. Biol.*, 2000, **7**, 127-133.
20. R. Y. N. Ho, M. P. Mehn, E. L. Hegg, A. Liu, M. J. Ryle, R. P. Hausinger and L. Que, Jr., *J. Am. Chem. Soc.*, 2001, **123**, 5022-5029.
21. M. P. Mehn, K. Fujisawa, E. L. Hegg and L. Que, Jr., *J. Am. Chem. Soc.*, 2003, **125**, 7828-7842.
22. E. G. Pavel, J. Zhou, R. W. Busby, M. Gunsior, C. A. Townsend and E. I. Solomon, *J. Am. Chem. Soc.*, 1998, **120**, 743-753.
23. R. E. Norman, R. Holz, S. Ménage, C. J. O'Connor and J. Q. Zhang, Jr., *Inorg. Chem.*, 1990, **29**, 4629-4637.
24. Y. M. Kim, K.-B. Cho, J. Cho, B. Wang, C. Li, S. Shaik and W. Nam, *J. Am. Chem. Soc.*, 2013, **135**, 8838-8841.
25. A. Company, I. Prat, J. R. Frisch, D. R. Mas-Ballesté, M. Güell, G. Juhász, X. Ribas, D. E. Münck, J. M. Luis, L. Que Jr. and M. Costas, *Chem. Eur. J.*, 2011, **17**, 1622-1634.
26. O. Planas, M. Clemancey, J.-M. Latour, A. Company and M. Costas, *Chem. Commun.*, 2014, **50**, 10887-10890.
27. C. V. Sastri, M. S. Seo, M. J. Park, K. M. Kim and W. Nam, *Chem. Commun.*, 2005, **11**, 1405-1407.
28. M. S. Seo, J.-H. In, S. O. Kim, N. Y. Oh, J. Hong, J. Kim, L. Que Jr. and W. Nam, *Angew. Chem. Int. Ed.*, 2004, **43**, 2417-2420.
29. M. Puri, A. Company, G. Sabenya, M. Costas and L. Que, Jr. *Inorg. Chem.*, 2016, **55**, 5818-5827.
30. I. Siewert and C. Limberg, *Angew. Chem. Int. Ed.*, 2008, **47**, 7953-7956.
31. K. Schröder, B. Join, A. J. Amali, K. Junge, X. Ribas, M. Costas and M. Beller, *Angew. Chem. Int. Ed.*, 2011, **50**, 1425-1429.
32. A. Gonzalez-de-Castro and J. Xiao, *J. Am. Chem. Soc.*, 2015, **137**, 8206-8218.

Graphical abstract

